

# Efficient, Dynamic Indexing and Aggregation of Moving Objects

SCOT ANDERSON and PETER REVESZ

University of Nebraska-Lincoln

---

We present novel Max-Count, Threshold-Range, Threshold-Count, Threshold-Sum, Threshold-Average and Count-Range estimation algorithms for dimensions based on a new spatiotemporal index. Each query runs in constant time and is based on a skew aware indexing technique with static size buckets. This allows constant time inserts, deletes and updates for highly dynamic spatiotemporal databases. The technique is also decomposable to allow partial results to be calculated simultaneously and recombined in linear time. We performed extensive experiments which show that the Max-Count estimation algorithm runs up to 35 times faster than a precise algorithm with accuracy above 95%.

Categories and Subject Descriptors: ... [...]: ...

General Terms: Algorithms, Experimentation

Additional Key Words and Phrases: Aggregation, Approximation, Databases, Indexing, Spatiotemporal

---

## 1. INTRODUCTION

Moving object databases naturally suggest new aggregate operators that have no equivalents in relational databases. For example, one may ask what is the maximum number of moving point objects that are simultaneously within a moving rectangular area at any time instance in a time interval  $T$ . This is called the Max-Count query. One may also ask during what time intervals in  $T$  are there more than  $M$  moving objects within a rectangle area. This is called a Threshold-Range. Alternatively, one may ask what is the number of moving objects that are within or intersect a rectangular area at any time instance in  $T$ . We call this the Count-Range query.

For Max-Count, there are only a few previous algorithms [Revesz and Chen 2003; Chen and Revesz 2004; Anderson 2006]. None of those previous algorithms are both efficient and dynamic. In this paper, we present the first efficient and dynamic algorithm for Max-Count. Table I compares the results of these earlier Max-Count algorithms with our current algorithm where  $N$  is the number of points and  $B$  is the number of buckets in the index.

---

This research was supported in part by NSF grant EIA-0091530 and a NASA Space and EPSCoR grant.

Permission to make digital/hard copy of all or part of this material without fee for personal or classroom use provided that the copies are not made or distributed for profit or commercial advantage, the ACM copyright/server notice, the title of the publication, and its date appear, and notice is given that copying is by permission of the ACM, Inc. To copy otherwise, to republish, to post on servers, or to redistribute to lists requires prior specific permission and/or a fee.

© 20YY ACM 0362-5915/20YY/0300-0001 \$5.00

Max. Dim.	Worst Case Time	Space	Exact or Estimation	Static or Dynamic	Reference
1	$O(\log N)$	$O(N^2)$	Exact	Static	[Revesz and Chen 2003]
1	$O(B \log B)$	$O(B)$	Estimation	Static	[Chen and Revesz 2004]
2	$O(B \log B)$	$O(B)$	Estimation	Static	[Anderson 2006]
d	$O(B)$	$O(B)$	Estimation	Dynamic	Current paper

Table I. Max-Count aggregation complexity on linearly moving objects.

Threshold-Range operators were not previously proposed for moving objects. To our knowledge we present the first such proposal. We also suggest additional variations on Threshold-Range that our operator is capable of returning. First we can return the total time instead of the time intervals which we call the Threshold-Sum. Second we can return the count of the number of congested areas encountered in the query which we call the Threshold-Count. Finally we can return the time that is the sum of the time intervals which we call Threshold-Sum.

Algorithms for spatiotemporal Range queries [Kollis et al. 1999; Saltenis et al. 2000; Porakaew et al. 2001; Papadopoulos et al. 2002] return the set of objects counted by the Count-Range query. These algorithms can be modified to return the Count-Range by counting the objects returned. Several other algorithms were proposed directly for the Count-Range problem in addition to the new algorithm proposed in this paper. We summarize previous spatiotemporal Range and Count-Range algorithms in Table II, where  $N$  is the number of moving objects or points in the database,  $d$  is the dimension of the space, and  $B$  is the number of buckets. All algorithms listed are dynamic, which means that they allow insertions and deletions of moving objects.

Max. Dim.	Worst Case Time	Worst case Space	Exact or Estimation	Reference
2	$O(N^{\frac{3}{4} + k})$	$O(N)$	Exact	[Kollis et al. 1999]
2	$O(\log_2 N + k)$	$O(N^2)^1$	Exact	
2	$O(N)$	$O(N)$	Exact	[Papadopoulos et al. 2002]
3	$O(N)$	$O(N)$	Exact	[Saltenis et al. 2000]
d	$O(N)$	$O(N)$	Exact	[Porakaew et al. 2001]
d	$O(B^{d-1} \log_B^d N)$	$O(\frac{N}{B} \log_B^{d-1} N)$	Exact	[Zhang et al. 2003]
2	$O(\log_B N + C) = B^2$	$O(N)$	Estimation	[Kollis et al. 1999]
2	$O(B)$	$O(B)$	Estimation	[Choi and Chung 2002]
d	$O(B)$	$O(B)$	Estimation	[Tao et al. 2003a] <sup>3</sup>
d	$O(\frac{N}{B})$	$O(N)$	Estimation	[Tao and Papadias 2005]
d	$O(B)$	$O(B)$	Estimation	Current Paper

Table II. Range and Count-Range Aggregation Summary

Max-Count, Threshold-Range and Count-Range are important in many applications such as tracking airplanes or mobile clients of wireless networks.

<sup>1</sup>This is a restricted future time query with expected  $O(N)$  space that becomes quadratic if the restriction is too far into the future.

<sup>2</sup> $C = K + K^0$ , where  $K^0$  is the approximation error.

<sup>3</sup>Although [Tao et al. 2003a] allows dynamic updates, over time the index must be rebuilt.

Example 1. Airplanes are commonly modeled as linearly moving objects with preestablished flight plans. Suppose at any time at most a constant  $M$  number of airplanes are allowed to be in the O'Hare airspace to avoid congestion. Suppose also a new airplane requests approval of its flight plan for entering the O'Hare airspace between times  $t_a$  and  $t_b$ . The air traffic controllers can avoid congestion as follows. If after adding a new flight plan the Max-Count between  $t_a$  and  $t_b$  is still less than  $M$ , then they can approve the flight. Otherwise, they need to find some alternative path and check it again against the database.

Air traffic controllers try to direct airplanes as linearly moving objects for fuel efficiency, among other reasons. If they recognize a developing congestion too late, then they often must direct the airplane to fly in circles until the congestion has cleared. That wastes fuel. On the other hand, if they recognize the developing congestion early, then they can often simply tell the airplane to change its speed, which saves fuel. Therefore, it is important to identify congestions as early as possible. That can be done by a Max-Count query where the query space is a moving box around the airplane and the time interval is  $[t_a; t_b]$ . If the Max-Count predicts congestion, then the airplane's speed can be adjusted early in the flight.

Example 2. Suppose we want to alert pilots if they are planning to fly through congested regions. The system that currently provides this functionality is known as a Traffic Alert/Collision Avoidance System (TCAS). Although TCASs were implemented in 1986, we have recently had mid-air collisions and near misses indicating that the system still needs improvement. Threshold-Range is a modification of Max-Count that returns all predicted (time, location) pairs where the Count exceeds a given threshold. This can be used to alert a pilot of predicted congestions where more than  $M$  other airplanes will be within the space  $B$  around the airplane. Predicting and avoiding these areas can significantly reduce the chances of mid-air collisions.

Example 3. Suppose we are especially concerned about a rush-hour period  $[t_a; t_b]$  that is particularly stressful to air traffic controllers. Suppose controllers can direct at most  $M$  airplanes safely. We can determine how many controllers are needed during the rush-hour time by executing the Count-Range query over the controlled airspace during the rush-hour and dividing by  $M$ . By ensuring that a sufficient number of controllers are present, safety is achieved and controllers are not overstressed.

There are other types of spatiotemporal aggregation besides the Max-Count, Threshold-Range and Count-Range operators. For example, [Agarwal et al. 2003; Tao and Papadias 2005; Bohlen et al. 2006] discussed other types of temporal and spatiotemporal aggregation dealing with discrete time events characterized by time stamps. Indexing and aggregation techniques related to exact sum, average or unique types of selection queries were given by [Tayeb et al. 1998; Zhang et al. 2001; Mokhtar et al. 2002; Revesz 2005]. Time parameterized minimum bounding boxes were discussed by [Cai and Revesz 2000; Pelanis et al. 2006; Saltenis et al. 2000]. Finally estimation techniques for aggregation as well as selectivity estimation were used in [Acharya et al. 1999; Gunopulos et al. 2005; Tao et al. 2003b; Wolfson and Yin 2003; Choi and Chung 2002; Tao et al. 2003b; Trajcevski et al. 2004; Kollios

et al. 2005]. Other interesting models for aggregation of moving objects within networks were given by [Gupta et al. 2004; Civilis et al. 2004; Civilis et al. 2005].

For more general discussion on spatial and spatiotemporal databases see the books [Guting and Schneider 2005; Rigaux et al. 2001; Samet 1990; 2005].

The rest of this paper is organized as follows. Section 2 introduces the skew-aware buckets used in the indexing methods. Section 3 gives the dynamic Max-Count algorithm and extensive details about its construction and execution. Section 4 introduces an exact Max-Count algorithm used for comparison with the estimated Max-Count. Section 5 gives our algorithm for the Count-Range query and shows that it is a simplification of the more general Max-Count query. Section 6 describes the Threshold-Range algorithm, its relationship to the Max-Count operator and suggests two other variations. Section 7 analyzes the accuracy and performance of the implementation of the exact and estimation Max-Count algorithms. Finally Section 8 gives conclusions and future work. In each section we describe the problems and solutions presented in one dimensional space for simplicity or three dimensional space where demonstrating aspects of higher dimensions is necessary.

## 2. DYNAMICALLY INDEXING LINEAR MOTION

Section 2.1 describes the problems related to creating hyper-buckets (also referred to as just buckets) and a specific solution for creating 6-dimensional buckets for 3-dimensional linearly moving points. In all cases we can extend our method to  $d$ -dimensions. Section 2.2 describes the method for inserting and deleting point from a bucket. Section 2.3 applies two different data structures to contain the buckets suited for applications where either inserts and deletes or Max-Count queries dominate.

### 2.1 HyperBuckets: Creating the buckets

**Definition 2.1.** Each 3-dimensional linearly moving point  $p$  can be described by parametric linear equations in  $t$  as follows:

$$p = \begin{pmatrix} x \\ y \\ z \end{pmatrix} = \begin{pmatrix} v_x t + x_0 \\ v_y t + y_0 \\ v_z t + z_0 \end{pmatrix}$$

The corresponding hex representation of  $p$  is the tuple  $(v_x; x_0; v_y; y_0; v_z; z_0)$ . For simplicity the six-tuple is often denoted  $(x_1; \dots; x_6)$ .

Consider a relation  $D(x_1; \dots; x_6)$  that contains the hex representation of linearly moving 3-dimensional points. Then  $D$  is a 6-dimensional static space. Divide the space into axis-aligned hypercubes. Each axis has  $d_k$  divisions and each face of a hyper-cube is parallel to some axis.

**Definition 2.2.** Each bucket  $B_i$  is described by inequalities of the form :

$$\begin{array}{llll} v_{x;L} & v_x < v_{x;U} & x_{0;L} & x_0 < x_{0;U} \\ v_{y;L} & v_y < v_{y;U} & y_{0;L} & y_0 < y_{0;U} \\ v_{z;L} & v_z < v_{z;U} & z_{0;L} & z_0 < z_{0;U} \end{array}$$

where we denote the lower and upper bounds as  $(v_{x;L}; x_{0;L}; v_{y;L}; y_{0;L}; v_{z;L}; z_{0;L})$  and  $(v_{x;U}; x_{0;U}; v_{y;U}; y_{0;U}; v_{z;U}; z_{0;U})$  respectively.

Each hyper-cube defines the spatial dimensions of a possible bucket, where only buckets that contain points are included in the index. The maximum number of possible buckets is given by  $m = \prod_{i=1}^d d_i$ .

**Definition 2.3.** Given a 6-dimensional bucket  $B_i$  containing  $b_i$  points, histograms  $h_{i,1}, \dots, h_{i,6}$  are built for each axis using  $s$  subdivisions as follows. To create histogram  $h_{i,j}$ , we divide bucket  $B_i$  into  $s$  parallel subdivisions along the  $j$ th axis and record separately the number of points within  $B_i$  that fall within each subdivision.

**Example 4.** Consider a set of 6-dimensional points projected onto the  $v_x; x_0$  plane as shown in Figure 1. Assume that the number of subdivisions is  $s = 10$ .

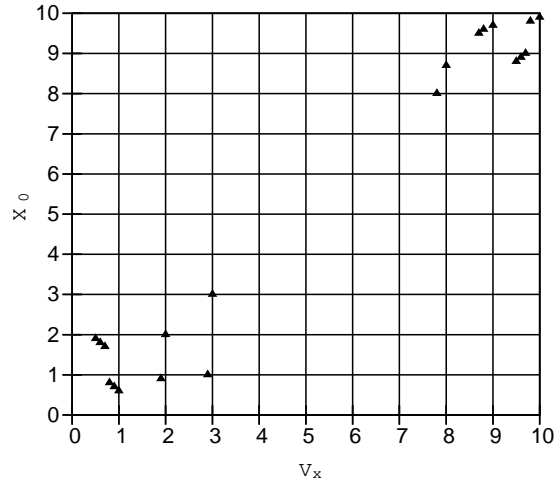


Fig. 1. Points projected onto  $v_x; x_0$  plane

along both  $v_x$  and  $x_0$ . Then Figure 2 shows  $h_{i,1}$  and  $h_{i,2}$ . For example, there are six points in the subdivision  $0 \leq v_x < 1$ , hence the first bar of histogram  $h_{i,1}$  rises to level 6. The other values can be determined similarly.

Histograms tell much about the distribution of the points in a bucket but they introduce some ambiguity. For example, the histograms in Figure 2 match both of the distributions in Figure 3.

**Definition 2.4.** The axis trend function  $f_{i,j}(x_j)$  is some polynomial function for bucket  $B_i$  and axis  $j$  such that the following hold:

- (1)  $f_{i,j} \geq 0$  over  $B_i$ .
- (2)  $f_{i,j}^0$ , the derivative  $f_{i,j}$ , does not change sign over the valid range.

The bucket trend function  $f_i$  for bucket  $B_i$  is the following:

$$f_i = \prod_j f_{i,j} \quad (1)$$

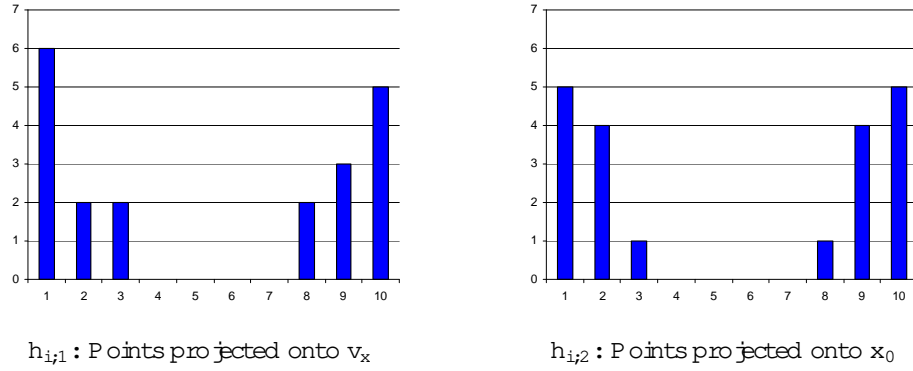


Fig. 2. Histogram of Points in 2 D in ensions

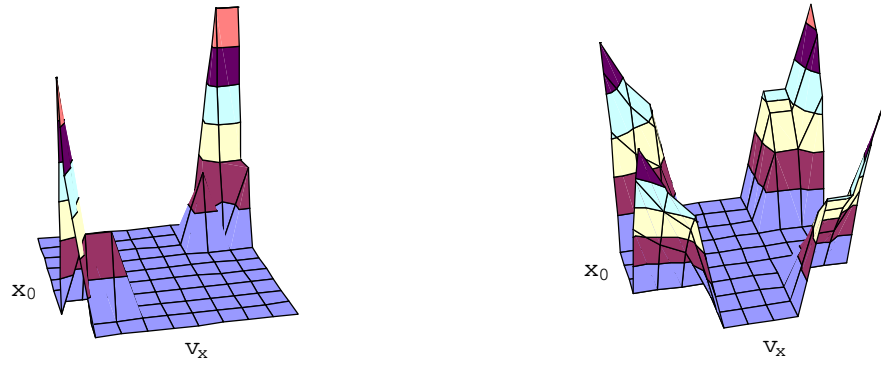


Fig. 3. 2D Distribution Functions

Condition 1 ensures that the bucket trend function built from the axis trend functions does not contain a negative probability region. Condition 2 requires that the bucket density increase, decrease or remain constant when considering any single axis. This smoothes out the bumps in the point density of the buckets and gives a polynomial which approximates the point density well.

Lemma 2.5. Given a bucket  $B_i$  with bucket trend functions  $f_{i,j}$ , let  $r_1$  and  $r_2$  be identically sized regions in bucket  $B_i$ . If the density in  $B_i$  along each axis monotonically increases from  $r_1$  to  $r_2$  the following holds:

$$\int_{r_2} f_i dZ \geq \int_{r_1} f_i dZ$$

Proof. Increasing densities from  $r_1$  to  $r_2$  translate into histograms that also increase from  $r_1$  in the direction of  $r_2$  along each axis. The translation from histograms to the axis trend functions gives the following conditions.

$$f_{i,j}(x_{2,j}) \geq f_{i,j}(x_{1,j})$$

where  $x_{1,j}$  and  $x_{2,j}$  are the  $j$  coordinate of points in  $r_1$  and  $r_2$  respectively and the points are located the same distance from the lower bounds of  $r_1$  and  $r_2$  respectively. Since this holds for each  $j$  and  $f_{i,j} = 0$  we have:

$$f_i(x_2) = f_i(x_1)$$

Hence by the properties of integration we conclude

$$\int_{r_2} f_i d = \int_{r_1} f_i d$$

□

Definition 2.4 allows a whole class of polynomial functions, and Lemma 2.5 applies to each member of that class. However, in the following we use a particular polynomial function derived from the product of linear functions, which are obtained by using the least square method for each histogram. This derivation is illustrated in Example 5.

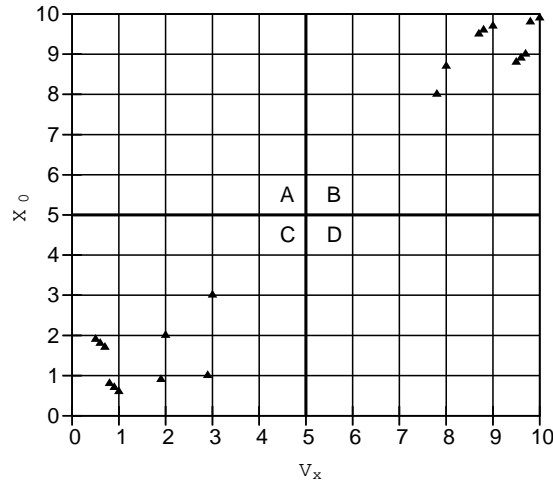


Fig. 4. Points projected onto  $v_x; x_0$  plane

Example 5. Split Figure 1 into 4 buckets as shown in Figure 4 and assume  $s = 5$ . Correspondingly, split Figure 2. Then each histogram becomes two histograms. For example, the left side from (0 to 5) of histogram  $h_{i,1}$  is the histogram for bucket C along the  $v_x$  axis. From the histograms build the axis trend functions along each axis for each bucket using the least squares method. From these build the bucket probability functions given by (1). Clearly for buckets A and D

$$f_A = 0$$

$$f_D = 0$$

To find a linear equation of the form  $y_i = ax_i + b$  where  $y_i$  is the approximated data and  $x_i$  is the point of subdivision, the least squares method results in two linear

equations called the normal equations:

$$\sum a \sum x_i^2 + b \sum x_i = \sum x_i y_i \quad (2)$$

$$\sum a \sum x_i + bN = \sum y_i \quad (3)$$

For bucket C and axis  $v_x$  the normal equations for least squares are:

$$55a + 15b = 16$$

$$15a + 5b = 10$$

Of course, the 55 and 15 will not change since we always have histograms numbered such that  $x_i = 1; \dots; 5$ . Solving these equations gives  $a = \frac{7}{5}$  and  $b = \frac{31}{5}$ . Hence the axis trend function for bucket C, axis  $v_x$  is

$$f_{C, v_x} = \frac{7}{5}v_x + \frac{31}{5}$$

Similarly for the  $x_0$  axis:

$$f_{C, x_0} = \frac{7}{5}x_0 + \frac{32}{5}$$

Since each function is decreasing, evaluate each function at the lower end point, 5 to ensure property (1) of Definition 2.4. Calculate  $f_{C, v_x}(5) = \frac{4}{5}$  and  $f_{C, x_0}(5) = \frac{3}{5}$ . Thus we must add  $\frac{4}{5}$  to each axis trend function and  $f_C$  is calculated using (1) as:

$$f_C = \frac{1}{25} (7v_x + 35) (7x_0 + 36) \quad (4)$$

Definition 2.6. Let  $n$  be the number of points in the database,  $b_i$  the number of points in bucket  $B_i$  and  $f_i$  be given by (1). The normalized trend function  $F_i$  for bucket  $B_i$  is:

$$F_i = \frac{b_i f_i}{\sum_{B_i} f_i d} \quad (5)$$

and the percentage of points in bucket  $B_i$  is:

$$p = \frac{F_i d}{B_i} \quad (6)$$

Example 6. Continuing from Example 5, integrating (4) over the bucket gives:

$$\int_0^5 \int_0^5 f_C dx_0 dv_x = \frac{1295}{4}$$

Given that  $\frac{b_i}{n} = \frac{1}{2}$ , calculating (5) for bucket  $B_C$  gives:

$$\begin{aligned} F_C &= \frac{1}{2} \frac{4}{1295} \frac{1}{5} (7v_x + 35) (7x_0 + 36) \\ &= \frac{2}{6475} (7v_x + 35) (7x_0 + 36) \end{aligned} \quad (7)$$



A similar process on bucket  $B_B$  gives:

$$F_B = \frac{4}{251850} (13v_x - 61)(13x_0 - 63) \quad (8)$$

Equations (7) and (8) are shown in Figure 5.

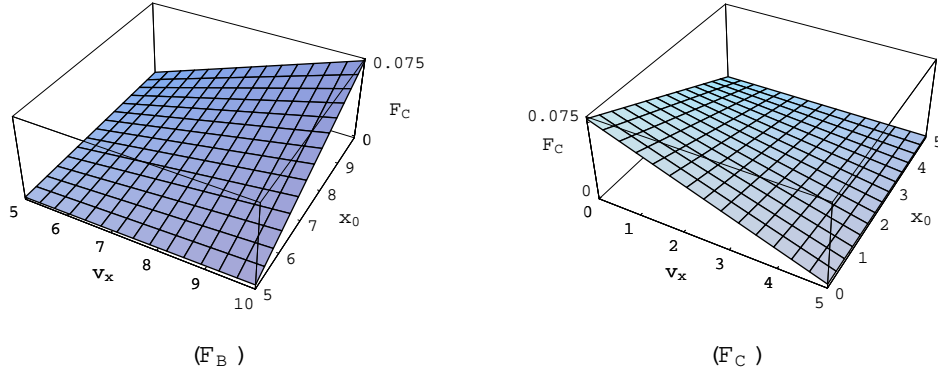


Fig. 5. Normalized trend functions in the  $v_x; x_0$  plane

Lemma 2.7. Let  $B_i$  be a bucket,  $n$  the number of points in the databases, and  $p$  be as defined in (6). Then  $np$  is the number of points in bucket  $B_i$ . Further,  $np$  can be calculated in  $O(1)$  time.

Proof. By (5) and (6) we have:

$$\begin{aligned} np &= n \sum_{B_i} F_i d \\ &= n \sum_{B_i} \frac{b_i \sum_{B_i} f_i}{n \sum_{B_i} f_i d} d \\ &= n \frac{b_i}{n} \frac{\sum_{B_i} f_i d}{\sum_{B_i} f_i d} \\ &= b_i \end{aligned}$$

It is easy to see that the above calculations take only  $O(1)$  time.  $\square$

## 2.2 Inserts and Deletes

It is possible to maintain the index while deleting or inserting a point for any bucket  $B_i$  by recalculating the trend function  $F_i$  for the bucket.

Lemma 2.8. Insertion and deletion of a moving point can be done in  $O(1)$  time.

**Proof.** When we insert or delete a point, we need to update the histograms and the normalized trend function. Let the point to insert/delete be  $P_a$  represented using the hex representation as  $(a_0; a_1; a_2; a_3; a_4; a_5)$ , let  $d_j$ , for each  $0 \leq j \leq 5$  be the width measured in buckets of the  $j^{\text{th}}$  dimension of the database, and let  $s$  be the number of subdivisions in each histogram. The ID, denoted  $ID_i$ , of bucket  $B_i$  to insert/delete  $P_a$  is given by the concatenation  $(id_0; \dots; id_6)$  where  $id_1$  is defined as  $id_1 = \frac{a_1}{d_1}$ . The calculation of  $ID_i$  and retrieving bucket  $B_i$  takes  $O(1)$  using a hashtable.

Let  $hw_{i,j}$  be the width of the  $j^{\text{th}}$  axis histogram calculated as  $hw_{i,j} = \frac{d_j}{s}$ . Then  $p$  is projected onto each dimension to determine which division of the histogram to update. For the  $j^{\text{th}}$  dimension the division  $k$  of histogram  $h_{i,j}$  is given as follows:

$$k(j) = \frac{a_j - id_j}{hw_k}$$

Let  $h_{i,j;k}$  be the histogram division to update for each histogram. Update  $h_{i,j;k}$  as well as  $y_i$  and  $x_i y_i$  from (2) and (3).  $N$ ,  $x_i$  and  $x_i^2$  do not need updating since the number of histogram divisions  $s$  is fixed within the database.

We can now recalculate each  $f_{i,j}$  in constant time by solving the  $2 \times 3$  matrix corresponding to (2) and (3) for each histogram. For each  $f_{i,j}$  calculate the endpoints to determine required shift amount (Definition 2.4, property 1) and calculate  $f_i$  from (1). Now we calculate  $F_i$  using (2.6). Each of these steps depends only on the dimension of the database. Hence for any fixed dimension we can rebuild the normalized trend function  $F_i$  in  $O(1)$  time.  $\square$

**Example 7.** Suppose we wish to delete point  $(0.9; 0.9)$  from the points shown in Figure 1. Calculating the ID gives Concatenate  $\frac{0.9-0}{1}; \frac{0.9-0}{1} = 00$  which is bucket C. Projecting this down onto the axes gives us the histogram  $sh_{0,v_x}$  and  $h_{0,x_0}$  on both axes:  $k(v_x) = \frac{0.9-0}{1} = 0$  and  $k(x_0) = \frac{0.9-0}{1} = 0$

Update the summation values indicated in Lemma 2.8 from equations (2) and (3) as:  $y_i = y_i - 1 = 9$  and  $x_i y_i = x_i y_i - 1 = 15$ . This gives us the following linear equations from (2) and (3).

$$55a + 15b = 15$$

$$15a + 5b = 9$$

Solving these gives  $a = -6/5$  and  $b = 27/5$ , and we obtain  $f_{C,v_0} = \frac{6}{5}v_x + \frac{27}{5}$ . Using a similar process gives  $f_{C,x_0} = \frac{6}{5}x_0 + \frac{28}{5}$ . Checking the endpoints shows that  $f_{C,v_0}(5) = 11.4$  is the smallest number. Adding 11.4 as a constant to  $f_{C,v_0}$  and  $f_{C,x_0}$  gives  $f_C$  as:

$$f_C = \frac{6}{25} (v_x + 14)(6x_0 + 85) \quad (9)$$

Integrating (9) over the bucket gives  $h = \int_0^5 \int_0^5 f_C dx_0 dv_x = 4830$ . Hence our recalculated normalized trend function for bucket C is:

$$F_C = \frac{2}{4025} (v_x + 14)(6x_0 + 85)$$

### 2.3 Index Data Structures

There is no need to create a bucket unless it contains at least one point. Consider two candidate data structures for organizing the buckets: hash tables and trees.

For databases where inserts and deletes are the most common operation, the hash table approach will allow these operations to run in constant time. However the Max-Count operation will require an enumeration of all the buckets and thus at least a running time of  $O(B)$ . As long as the number of buckets is reasonable this approach works well.

For databases where Max-Count is the most common operation, use an R-tree type structure [Guttman 1984; Beckmann et al. 1990] where the elements to be inserted are the buckets. This speeds up the Max-Count query to  $O(\log B + R)$  where  $R$  is the number of buckets needed to calculate the query. The insert and delete costs for these R-trees are  $O(\log B)$ , because buckets do not overlap.

Since buckets do not change shape, the database is decomposable and allows each type of aggregation to be calculated from simultaneous executions on subspaces of the index space. We discuss the method and ramifications of this capability at the end of Section 4.

## 3. DYNAMIC MAX-COUNT

Section 3.1 reviews point domination in higher dimensions. Section 3.2 examines finding the percentage of points in a bucket that are in the query space as a function of time. Section 3.3 puts all this together to create the dynamic Max-Count algorithm for  $d$ -dimensions.

### 3.1 Point Domination in 6-Dimensional Space

Let  $B$  be the set of 6-dimensional hyper-buckets in the input where each hyper-bucket  $B_i$  has an associated normalized trend function  $F_i$  as in Definition 2.6. Let the vertices of  $B_i$  be denoted  $v_{i,j}$  where  $1 \leq j \leq 64$ , because there are  $2^6$  corner vertices to a 6-dimensional hyper-cube.

Definition 3.1. Given two linearly moving points in three dimensions

$$P(t) = \begin{pmatrix} p_x \\ p_y \\ p_z \end{pmatrix} = \begin{pmatrix} x_1 t + x_2 \\ x_3 t + x_4 \\ x_5 t + x_6 \end{pmatrix} \quad \text{and} \quad Q(t) = \begin{pmatrix} q_x \\ q_y \\ q_z \end{pmatrix} = \begin{pmatrix} v_x t + x_0 \\ v_y t + y_0 \\ v_z t + z_0 \end{pmatrix}$$

$Q(t)$  dominates  $P(t)$  if and only if the following holds:

$$\overset{\wedge}{p_x} < \overset{\wedge}{q_x} \quad \overset{\wedge}{p_y} < \overset{\wedge}{q_y} \quad \overset{\wedge}{p_z} < \overset{\wedge}{q_z}$$

The previous Definition takes 6-dimensional points defined in Definition 2.1 and places them into three inequalities of the form  $x_2 < t(x_1 - v_x) + x_0$ . Each inequality defines a region below a line with slope  $-t$ .

Definition 3.2. Projecting the inequalities from Definition 3.1 onto their respective dual planes allows a visualization in three 2-dimensional planes. Define these three projections as the *x view*, *y view* and *z view* respectively. Because the time  $t$  defines the slopes of each line, all views contain lines with identical slopes.

**Definition 3.3.** Given two moving query points  $Q_1(t)$  and  $Q_2(t)$  and lines  $l_{x1}, l_{x2}, l_{y1}, l_{y2}, l_{z1}, l_{z2}$  crossing them in their respective hexes with slopes  $t$ , the intersection of the bands formed by the area between  $l_{x1}$  and  $l_{x2}$ ,  $l_{y1}$  and  $l_{y2}$ , and  $l_{z1}$  and  $l_{z2}$  in the 6-dimensional space forms a hyper-tunnel that is the query space as shown in Figure 6.

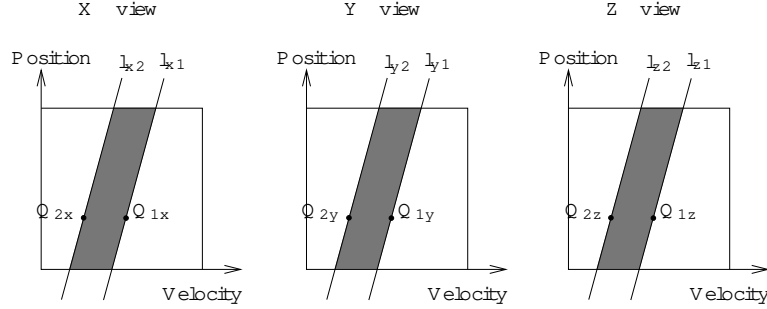


Fig. 6. Views

We can now visualize the query in space and time as the query space sweeping through a bucket as the slopes of the lines change with time. Using the above it is now easy to prove the following lemma.

**Lemma 3.4.** At any time  $t$  the moving points whose hex-representation lie below (or above)  $l_{x1}; l_{y1}$  and  $l_{z1}$  in their respective views are exactly those points that lie below (or above)  $Q_1$  in the original 3-dimensional plane.

**Proof.** Let  $Q_x(t) = v_x t + x_0$  where  $v_x$  and  $x_0$  are constants and consider any  $x$  component of a point  $P_x(t) = x_1 t + x_2$  that lies below  $Q$  on the  $x$ -axis. Then

$$\begin{aligned} x_1 t + x_2 &< v_x t + x_0 \\ x_2 &< t(x_1 - v_x) + x_0 \end{aligned}$$

Obviously, at any time  $t$  these are the points below the line  $x_2 = t(x_1 - v_x) + x_0$  which has a slope of  $t$  and goes through  $(v_x; x_0)$ . This is the dual of point  $Q_x$ . By Definition 3.3 this is exactly the line  $l_{x1}$ . We can prove similarly that the points with duals above  $l_{x1}$  are above  $Q_1$  at any time  $t$ . The proof that points whose hex-representations are above or below  $l_{y1}$  and  $l_{z1}$  are exactly those points that lie above or below  $Q_1$  is similar to the proof for points above or below  $l_{x1}$ . By Definition 3.1, we conclude that the points dominated by  $Q_1$  in the dual space are those points that are below  $l_{x1}; l_{y1}$  and  $l_{z1}$  in the  $x$ -view,  $y$ -view and  $z$ -view, respectively. Similarly, we conclude that the points that dominate  $Q_1$  in the dual space are those points that are above  $l_{x1}; l_{y1}$  and  $l_{z1}$  in the  $x$ -view,  $y$ -view and  $z$ -view, respectively.  $\square$

Throughout the examples in this section we use the points shown in Figures 7 and 8 to demonstrate the evaluation of a Max-Count query. We begin by creating the index.

ID	Dimension 1		Dimension 2		Dimension 3	
	X0	X1	X2	X3	X4	X5
1	5.345	7.543	5.345	8.158	5.345	5.488
2	6.354	9.023	6.354	5.488	6.354	5.159
3	7.159	8.885	7.159	6.685	7.159	7.346
4	7.645	9.117	7.645	5.159	7.645	8.885
5	8.153	7.346	8.153	6.335	8.153	7.543
6	8.156	6.335	8.156	7.346	8.156	9.023
7	9.125	5.159	9.125	9.117	9.125	9.117
8	9.118	6.685	9.118	8.885	9.118	6.335
9	9.688	5.488	9.688	9.023	9.688	8.158
10	9.874	8.158	9.874	7.543	9.874	6.685

Fig. 7. Example Points

## Example 8. Estimated Max-Count Calculation

**Index Creation:** Consider a relation containing a 6-dimensional space 10 units (0:::10) in each dimension. If we break this up into buckets that are 5 units long in each dimension, we have  $2^6$  buckets. Although this makes a space with 64 buckets, all the points are contained in a single bucket whose index is (2;2;2;2;2;2). The points listed in Figure 7 all have the same velocities for each dual plane. Notice the columns for  $x_1$ ,  $x_3$  and  $x_5$  all have the same values in different orders. The projection of the points onto the 3 dual planes shown in Figure 8 does not immediately show this organization. Projecting the points onto each axis and creating

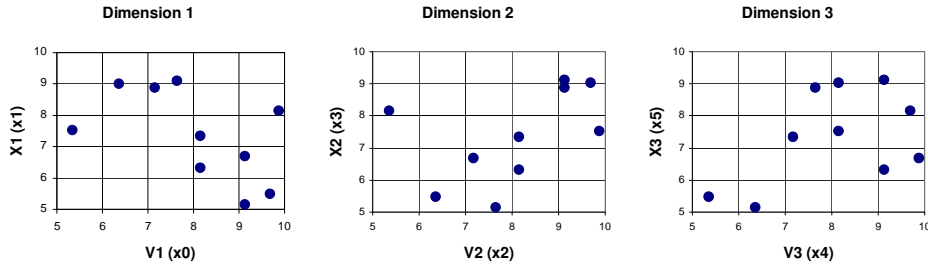


Fig. 8. Points P projected onto the Three Dual Planes

histograms with 5 divisions is shown for the Velocity and Position axes in Figure 9. Each velocity dimension has the same histogram and similarly each position dimension has the same histogram. The histograms for velocity and position in each view are given as: Velocity =  $f(5;1); (6;1); (7;2); (8;2); (9;4)g$  and Position =  $f(5;2); (6;2); (7;2); (8;2); (9;2)g$ . Using the least squares method to fit each of

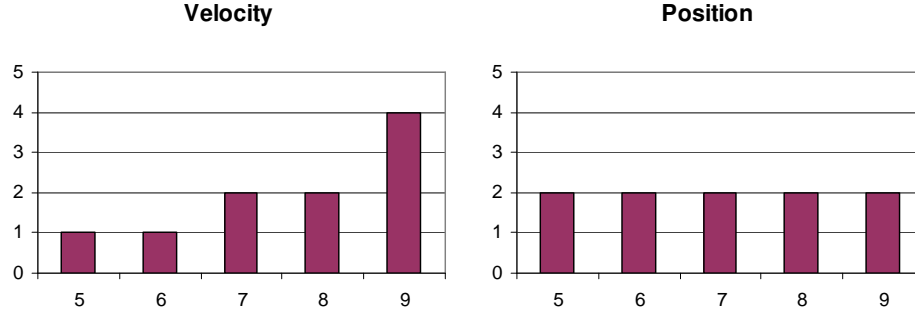


Fig. 9. Velocity and Position Histograms

these to a line gives the following for each velocity and position dimension:

$$\text{Velocity : } y = 0.7x - 2.9 \quad (10)$$

$$\text{Position : } y = 0x + 2 \quad (11)$$

Evaluating (10) and (11) at the end points to find the shift value for the axis trend function to add to each equation gives:

$$\text{Velocity : } y(5) = 1; \quad y(10) = 4.3$$

$$\text{Position : } y(5) = y(10) = 2$$

Hence in this case no constant needs to be added to our equation, and the trend function becomes:

$$f_i = (0.7x_0 - 2.9)(0x_1 + 2)(0.7x_2 - 2.9)(0x_3 + 2)(0.7x_4 - 2.9)(0x_5 + 2) \quad (12)$$

Calculating  $F_i$  from (5) requires integrating  $f_i$  over the bucket where  $R_{B_i} \dots R_{10}$  and where  $dZ = dx_0 dx_1 dx_2 dx_3 dx_4 dx_5$  gives

$$\begin{aligned} \int_{B_i} f_i dZ &= \int_{B_i} (0.7x_0 - 2.9)(0.7x_2 - 2.9)(0.7x_4 - 2.9) dZ \\ &= 1622234.375 \end{aligned}$$

Since all the points reside in a single bucket,  $b_i = n$ , the constant  $c$  is given by  $c = 1/1622234.375 \cdot 6.164 \cdot 10^{-7}$ . Then  $F_i$  is given by

$$\begin{aligned} F_i &= c (0.7x_0 - 2.9)(0x_1 + 2)(0.7x_2 - 2.9)(0x_3 + 2)(0.7x_4 - 2.9)(0x_5 + 2) \\ &= 8c(0.7x_0 - 2.9)(.7x_2 - 2.9)(.7x_4 - 2.9) \end{aligned}$$

So far we have come up with the normalized trend function  $F_i$  for just one bucket. This finishes the index creation process where the index contains a single bucket defined by lowerbound = (5;5;5;5;5;5) and upperbound = (10;10;10;10;10;10).

### 3.2 Approximating the Number of Points in a Bucket

As a line through a query point sweeps across a bucket, the points in the bucket that dominate the query point are approximated by the integral over the region

above the line. In each of the three views the query space intersects the plane giving the cases shown in Figure 10.

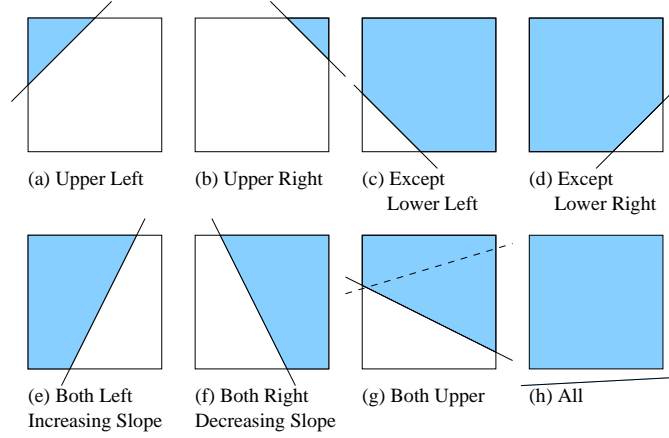


Fig. 10. Sweep Algorithm Cases

**Definition 3.5.** Integrating over the region above the line gives an approximation of the percentage of points in the query space. We define the percentage function given as:

$$p = \frac{\int_{r_1}^Z F_i d}{Z} \quad (13)$$

where  $r_1$  is the region of the bucket in the query space. If two lines go through the same bucket we have the smaller region  $r_2$  subtracted from the larger region  $r_1$  as follows.

$$4p = \frac{\int_{r_1}^Z F_i d}{Z} - \frac{\int_{r_2}^Z F_i d}{Z} \quad (14)$$

Here regions  $r_1$  and  $r_2$  correspond to regions above  $Q_1$  and  $Q_2$  in Figure 6, respectively. Finding the number of points in the bucket requires multiplying (13) by  $n$ .

For each case shown in Figure 10, we describe the function that results from integration in one view. To extend the result to any number of views, we take the result from the last view and integrate it in the next view. If the region below the line were desired,  $p_{lower} = \frac{b_i}{n} p$  gives the percentage of points below the line.

For cases (a)–(h) below, let  $Q = (x_{1,q}; x_{2,q}; \dots; x_{6,q})$ . For the  $x$ -view, let the lower left corner vertex be  $(x_{1,l}; x_{2,l})$  and the upper right corner vertex be  $(x_{1,u}; x_{2,u})$ . In addition each line denoted  $l$  is  $x_2 = t(x_1 - x_{i,q}) + x_{i+1,q}$  and corresponds to the lines shown in the corresponding case in Figure 10.

Case (a): For this case  $l$  crosses the bucket at  $x_{1;l}$  and  $x_{2;u}$ . The integral over the shaded region is given by the following:

$$p_a = \int_{x_{1;l}}^{\frac{x_{2;u} - x_{2;q}}{t} + x_{1;q}} \int_{x_{2;u}}^{\infty} F_i dx_2 dx_1 \quad (15)$$

Notice that the lower bound of the integral over  $dx_2$  contains  $x_1$ . This dependence within each view does not affect the integration in the remaining four dimensions. The solution to (15) has the form:

$$at^2 + bt + c + \frac{d}{t} + \frac{e}{t^2} \quad (16)$$

Case (b): For this case  $l$  crosses the bucket at  $x_{1;u}$  and  $x_{2;u}$ . The integral over the shaded region is given by:

$$p_b = \int_{\frac{(x_{2;u} - x_{2;q})}{t} + x_{1;q}}^{\infty} \int_{x_{2;u}}^{\infty} F_i dx_2 dx_1 \quad (17)$$

The solution has the form of (16).

Case (c): For this case  $l$  crosses the bucket at  $x_{1;l}$  and  $x_{2;l}$ . The integral over the shaded region above the line is given by:

$$p_c = \int_{x_{1;l}}^{\frac{x_{2;l} - x_{2;q}}{t} + x_{1;q}} \int_{x_{2;l}}^{\infty} F_i dx_2 dx_1 + \int_{\frac{x_{2;l} - x_{2;q}}{t} + x_{1;q}}^{\infty} \int_{x_{2;l}}^{\infty} F_i dx_2 dx_1 \quad (18)$$

The solution has the form of (16).

Case (d): For this case  $l$  crosses the bucket at  $x_{1;u}$  and  $x_{2;l}$ . The integral over the shaded region is given by:

$$p_d = \int_{\frac{x_{2;l} - x_{2;q}}{t} + x_{1;q}}^{\infty} \int_{x_{2;l}}^{\infty} F_i dx_2 dx_1 + \int_{x_{1;u}}^{\frac{x_{2;l} - x_{2;q}}{t} + x_{1;q}} \int_{x_{2;l}}^{\infty} F_i dx_2 dx_1 \quad (19)$$

The solution has the form of (16).

Case (e): For this case  $l$  crosses the bucket at  $x_{1;l}$  and  $x_{1;u}$ . The integral over the shaded region is given by:

$$p_e = \int_{x_{2;l}}^{\frac{x_{2;u} - x_{2;q}}{t} + x_{1;q}} \int_{x_{1;l}}^{\infty} F_i dx_1 dx_2 \quad (20)$$

The solution has the form of

$$c + \frac{d}{t} + \frac{e}{t^2} \quad (21)$$



which is like (16) with  $a = b = 0$ .

Case (f): Similar to case (e),  $l$  crosses the bucket at  $x_{1,l}$  and  $x_{1,u}$ . The integral over the shaded region is given by:

$$p_d = \int_{x_{2,l}}^{x_{2,u}} \int_{\frac{x_2 - x_{2,q}}{t} + x_{1,q}}^{x_{1,u}} F_i dx_1 dx_2 \quad (22)$$

The solution has the form of (21).

Case (g): For this case  $l$  crosses the bucket at  $x_{1,l}$  and  $x_{1,u}$ . The integral over the shaded region is given by:

$$p_g = \int_{x_{1,l}}^{x_{1,u}} \int_{t(x_1 - x_{1,q}) + x_{2,q}}^{x_{2,u}} F_i dx_2 dx_1 \quad (23)$$

The solution has the form

$$at^2 + bt + c \quad (24)$$

which is like (16) with  $d = e = 0$ .

Case (h): The line  $l$  crosses below all the corner vertices so the integral of the function is given as:

$$p_h = \int_{x_{1,l}}^{x_{1,u}} \int_{x_{2,l}}^{x_{2,u}} F_i dx_2 dx_1 \quad (25)$$

The solution has the form of (24).

The above cases have solutions for each view in the form of (16). Hence the percentage function for a single bucket as a function of  $t$  is of the form :

$$p = a_x t^2 + b_x t + c_x + \frac{d_x}{t} + \frac{e_x}{t^2} + a_y t^2 + b_y t + c_y + \frac{d_y}{t} + \frac{e_y}{t^2} + a_z t^2 + b_z t + c_z + \frac{d_z}{t} + \frac{e_z}{t^2} \quad (26)$$

where  $t \neq 0$  when  $d_x; d_y; d_z; e_x; e_y; e_z \neq 0$ . Finally, renaming variables gives the general form :

$$p = a_6 t^6 + a_5 t^5 + a_4 t^4 + a_3 t^3 + a_2 t^2 + a_1 t + c + \frac{d_1}{t} + \frac{d_2}{t^2} + \frac{d_3}{t^3} + \frac{d_4}{t^4} + \frac{d_5}{t^5} + \frac{d_6}{t^6} \quad (27)$$

where  $t \neq 0$  when  $d_i \neq 0$  for  $1 \leq i \leq 6$ . Since (27) is closed under subtraction, 4  $p$  from (14) will also have the same form.

As the query space from Definition 3.3 sweeps through a bucket, it crosses the bucket corner vertices. Each time a corner vertex crosses the query space boundary, the case that applies may change in one or more of the views.

Definition 3.6. A bucket time interval is defined as the span of time in which no vertex from bucket  $B_i$  enters or leaves the query space. The bucket time interval is

denoted as  $[l;u)$  where  $l$  is the lower bound and  $u$  is the upper bound. Each bucket time interval has an associated percentage function  $\phi_p$  given by (14). We define the index time interval similarly except that the span of time is defined when no vertex from any bucket in the index enters or leaves the query space.

As we will see, index time intervals are created from individual bucket intervals. Throughout the rest of this paper we use time intervals when the context clearly identifies which type we mean.

**Definition 3.7.** Let  $B$  be the set of buckets. Let  $Q_1$  and  $Q_2$  be two query points and  $(t^l; t^u)$  be the query time interval. We define the Time Partition Order to be the set of ordered time instances  $TP = t_1; t_2; \dots; t_i; \dots; t_k$  such that  $t_1 = t^l$  and  $t_k = t^u$ , and each  $[t_i; t_{i+1})$  is an index time interval.

**Example 9.** Continuing Example 8, let  $Q$  be a query defined by:

$$\begin{aligned} q_1 &= (9.5; 8; 9.5; 8; 9.5; 8) \\ q_2 &= (8.5; 5; 8.5; 5; 8.5; 5) \\ T &= (0.1; 10) \end{aligned}$$

where  $q_1$  and  $q_2$  form the query space over the query time interval  $T$ . To determine time intervals when corner vertices do not change, find the slopes of lines through both query points and each corner vertex of the bucket. Figure 11 shows lines from the two query points to the corner vertices for the first dimension. Since the query points are the same in each dimension each will appear the same. This is shown in Figure 11. The times when lines through  $q_1$  (shown as solid lines) cross corner

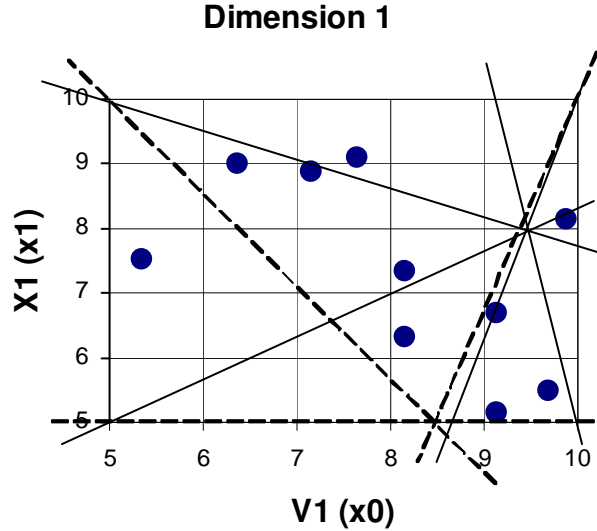


Fig. 11. Lines from Query Points to Corner Vertices

vertices are  $f(0.4; 6)g$ . The times  $q_2$  (shown as dotted lines) cross corner vertices are  $f(1.42857)g$ . The union of these two along with the end points makes up the times used to create the time intervals:  $f(1; 0.4); (0.4; 1.42857); (1.42857; 6); (6; 10)g$ .

Integration over the spatial dimensions of the eight possible cases presented in Figure 10 gave a function of the form of (27). Maximizing (27) in the temporal dimension by first taking the derivative, we get:

$$4p^0 = (6a_6t^{12} + 5a_5t^{11} + 4a_4t^{10} + 3a_3t^9 + 2a_2t^8 + a_1t^7 - d_1t^5 - 2d_2t^4 - 3d_3t^3 - 4d_4t^2 - 5d_5t - 6d_6)t^7 \quad (28)$$

where  $t \in \mathbb{R}$ . Solving  $p^0 = 0$  requires finding the roots of this 12-degree polynomial which is not possible using an exact method. This requires a numerical method for solving the polynomial.

The following factors influenced the choice of the numerical method:

- (1) Speed of the algorithm is more important than accuracy because we don't expect the original function to change dramatically over an index time interval.
- (2) The algorithm must converge toward a solution within the interval, that is the algorithm must be stable.
- (3) Given that we are maximizing (27) over a short time interval, we don't expect (28) to have more than one solution. This may seem naive, but it is reasonable given factor (1).

Factor (1) above is related to (3) in that it indicates that points close together have similar values, but emphasizes that speed is the goal. Factor (2) above eliminates several algorithms from consideration, but must be required to keep from choosing a solution that is not within the time interval evaluated.

Of the three points to consider, (3) is probably the least intuitive. Consider the following Lemma:

**Lemma 3.8.** Given  $p$  for a set of buckets, if the Euclidean distance between two maximums is small, then the difference between the maximums is small.

**Proof.** Consider the physical characteristics of the system. The change in  $p$  over the time interval is no more than  $b_i$  for any bucket  $B_i$ . Clearly  $p$  is either increasing as it encompasses more of the bucket or decreases as it encompasses less of the bucket. When  $p$  represents the distribution over several buckets, each bucket contributes a decreasing or increasing amount over the time interval. Clearly change in  $p$  is bounded below by 0 and above by  $b_i$ . Hence the rate at which  $p^0$  changes is characterized by the physical system and reflects the differences in the buckets as  $t$  changes. Since  $p$  does not change dramatically over  $t$  for any bucket, then change in several buckets over  $t$  will likewise not be dramatic. Hence if the distance between two maximums is small, the maximums have a small difference in magnitude.  $\square$

Based on these factors we use a well known concept (known as the bisection method) for the first approximation: look at the graph. Programmatically check  $c$  intervals of (28) for a change in sign. If there exists a sign change, use the bisection

method to find the root. If two points lie within  $\epsilon$  of 0, perform an additional check for each of these intervals when no change of sign is found. If some roots exist check them for maximal values along with the end points.

**Lemma 3.9.** The approximate maximum within a time interval can be found in  $O(1)$  time.

**Proof.** Each time interval has an associated probability function  $4p$  which is calculated in  $O(1)$  time. Finding  $4p^0 = 0$  also takes  $O(1)$  time. By placing a constant bound on the number of iterations in the bisection method, we bound the time required in the numerical section of the algorithm by a constant. Plugging in the solution found by the bisection method along with the end points also takes  $O(1)$  time. Hence the running time to find the maximum within a bucket is  $O(1)$ .  $\square$

We chose to limit the number of iterations in the bisection method to 10 which limits the running time to a small constant value. This value was chosen based on the index time intervals being small (about 0.01 to 4). Using the bisection method allows us to narrow our search down to an interval at least as small as 0.003 units of time.

**Example 10.** Continuing Example 9 we build the functions for time intervals  $f([1;0.4]; (0.4;1.42857]; (1.42857;6); (6;10)g$  by integrating using the different cases from Figure 10.

**Time Interval:**  $[0;1;0.4]$ . Here case (c) holds for query point  $q_2$  over this time interval. Hence the integral for query point  $q_2$  and  $t \in [1;4]$  in each dimension is given as:

$$\begin{aligned} p_e &= c \int_{8.5}^{10} \int_{5}^{10} 2(0.7x_0 - 2.9)dx_1 dx_0 + \int_{8.5}^{10} \int_{5}^{10} 2(0.7x_0 - 2.9)dx_1 dx_0 \\ &= 117.5 - 17.3546t \end{aligned} \quad (29)$$

Case (g) holds for query point  $q_1$  and thus the integral for query point  $q_1$  and  $t \in [1;4]$  in each dimension is given as:

$$\begin{aligned} p_g &= c \int_{5}^{10} \int_{5}^{10} 2(0.7x_0 - 2.9)dx_1 dx_0 \\ &= 47.0 - 32.416t \end{aligned}$$

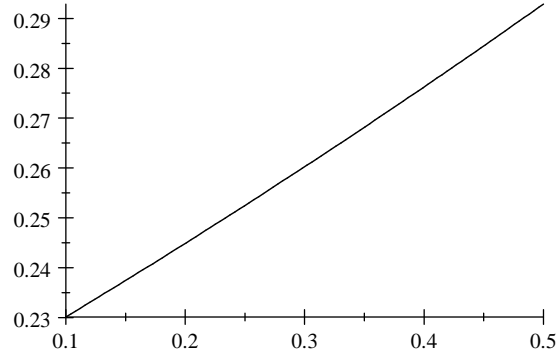
Hence the integral of the region is:

$$\begin{aligned} p &= c (p_e - p_g)^3 \\ &= 2.106 - 10^{-3}t^3 + 2.957 - 10^{-2}t^2 + 0.138t + 0.216 \end{aligned}$$

Evaluating  $p$  at the start and end of the time interval we have  $p(0.1) = 0.23$  and  $p(0.4) = 0.28$ . Figure 12 shows  $p$  in the time interval. Clearly  $p$  is increasing, so that we have a maximum at the end point  $t = 0.4$ . Since there are 10 points we must multiply  $p(0.4)$  by 10 to get the approximation for the time interval as:

$$\text{MaxCount}_{0.1 \leq t \leq 0.4} = 2.8$$

Since we can not have partial points, we can round this to 3.

Fig. 12. Graph of  $p, 0.1 \leq t \leq 0.4$ 

Time Interval  $[0.4; 1.428]$ . Note that case (c) holds for query point  $q_2$  over this time interval, hence  $p_e$  is given in (29). Case (b) holds for  $q_1$  over this interval. Therefore,

$$\begin{aligned}
 p_b &= \int_{\frac{(10-8)}{t} + 9.5}^{Z_{10}} \int_{t(x_0 - 9.5) + 8}^{Z_{10}} (0.7x_0 - 2.9)(2) dx_1 dx_0 \\
 &= 0.9953t + \frac{15}{t} - \frac{1.86}{t^2} + 7.85
 \end{aligned} \tag{30}$$

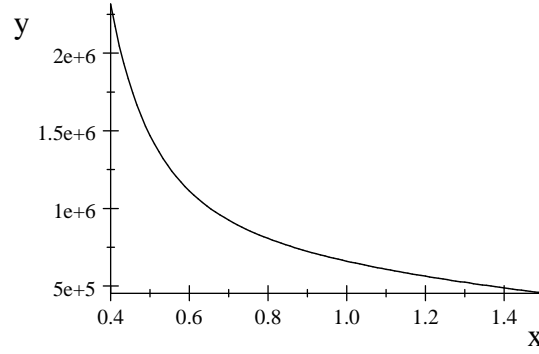
Hence the integral over the region is

$$\begin{aligned}
 p &= c(p_e - p_b)^3 \\
 &= \frac{8.902}{t^2} - \frac{0.355}{t} + 0.417t + 6.827 - \frac{10^{-2}t^2}{t^3} + \frac{1.355}{t^3} - \frac{10^{-2}}{t^3} \\
 &\quad + 3.808 - \frac{10^{-3}t^3}{t^4} + \frac{1.483}{t^4} - \frac{9.665}{t^5} + \frac{4.009}{t^6} - \frac{10^{-6}}{t^6} + 0.925
 \end{aligned}$$

Checking the values gives  $p(0.4) = 0.28$  and  $p(1.428) = 0.248$ . Neither of these produce values larger than our current maximum. The graph of  $p$  in Figure 13 shows that there is no interior maximum.

Time Interval  $[1.42857; 6]$ . Note that case (b) holds for query point  $q_1$  over this time interval, hence  $p_b$  is given in (30). Case (f) holds for  $q_2$  over this interval. Therefore,

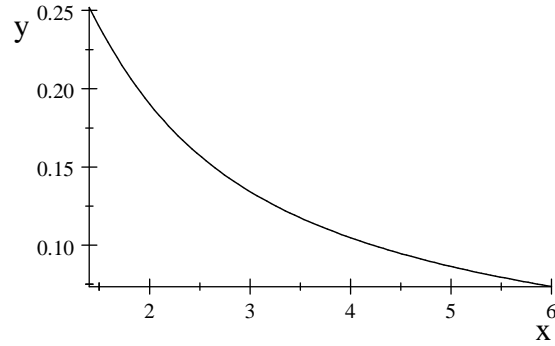
$$\begin{aligned}
 p_d &= \int_{\frac{(x_1 - 5)}{t} + 8.5}^{Z_{10}} \int_{Z_{10}} (0.7x_0 - 2.9)(2) dx_0 dx_1 \\
 &= 53.625 + \frac{76.25}{t} - \frac{29.166}{t^2}
 \end{aligned} \tag{31}$$

Fig. 13. Graph of  $p, 0.4 \leq t \leq 1.428$ 

Hence the integral is given by:

$$\begin{aligned}
 p &= c(p_d - p_o)^3 \\
 &= \frac{0.235}{t} - 3.746 \cdot 10^{-3}t + \frac{0.217}{t^2} + 8.395 \cdot 10^{-5}t^2 - \frac{0.143}{t^3} - 6.088 \cdot 10^{-7}t^3 \\
 &\quad + \frac{0.126}{t^4} + \frac{8.442 \cdot 10^{-2}}{t^5} - \frac{1.254 \cdot 10^{-2}}{t^6} + 4.875 \cdot 10^{-2}
 \end{aligned}$$

As shown in Figure 14, we again have a decreasing function which has no interior maximums. Evaluating  $p$  at the end points gives  $p(1.428) = 0.248$  and  $p(6) = 0.073$ . Therefore we keep our current maximum.

Fig. 14. Graph of  $p, 1.428 \leq t \leq 6$ 

Time Interval  $[6; 10]$  Case (f) holds for both query points. Equation (31) gives

the integral for  $q_2$ . The integral for  $q_1$  is given as:

$$\begin{aligned} p_{dq_1} &= \int_5^{10} \int_{\frac{(x_1-8)}{t} + 9.5}^{10} (0.7x_0 - 2.9)(2) dx_0 dx_1 \\ &= 19.625 - \frac{8.167}{t^2} - \frac{18.75}{t} \end{aligned}$$

Therefore the integral is given by:

$$p = c(p_{dq_2} - p_{dq_1})^3 = 2.42 \cdot 10^{-2} + \frac{0.203}{t} + \frac{0.523}{t^2} + \frac{0.278}{t^3} - \frac{0.323}{t^4} + \frac{7.748}{t^5} - \frac{5.709}{t^6} \cdot 10^{-3}$$

As shown in Figure 15 we again have a decreasing function which has no interior

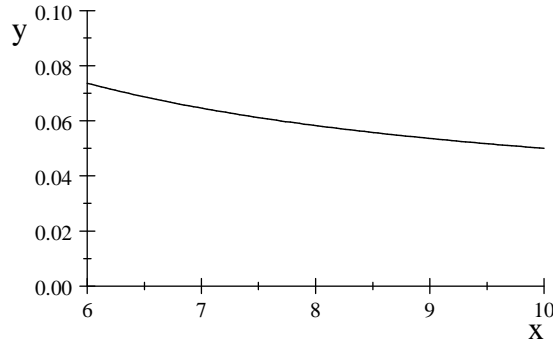


Fig. 15. Graph of  $p, 6 \leq t \leq 10$

maximums. Evaluating  $p$  at the end points gives  $p(6) = 0.0736$  and  $p(10) = 0.05$ . Therefore we keep our current maximum.

**Max-Count and Time:** From the above, it follows that Max-Count has an approximate value of 3 at time  $t = 0.4$ .

### 3.3 Dynamic Max-Count Algorithm

The algorithm to compute Max-Count with each line labeled with its running time is the following:

---

Max-Count( $H; Q_1; Q_2; t^l; t^h$ )

input: A set of buckets  $H$  built by the index structure presented,  
 query points  $Q_1(t)$  and  $Q_2(t)$  and a query time interval  $(t^l; t^h)$ .  
 output: The estimated Max-Count value.

```

01. TimeIntervals = ;                                O (1)
02. for i= 0 to |H| - 1                               O (B)
03.   CrossTimes = CalculateCrossTimes( $Q_1; Q_2; t^l; t^h; H_i$ )  O (1)
04.   for each j= 1 to |CrossTimes| - 1                O (1)
05.     Union(TimeIntervals; TimeInterval( $t_{j-1}; t_j$ ))  O (1)
06.   end for
07. end for

08. TimeIntervals = BucketSort(TimeIntervals)          O (B)
09. IndexTimeIntervals = Merge(TimeIntervals)          O (B)
10. for each IndexTimeInterval2 IndexTimeIntervals    O (B)
11.   calculate(MaxCount; MaxTime; IndexTimeInterval)  O (1)
12. end for

13. return (MaxCount; MaxTime)

```

---

Line 01 initiates a set of bucket time interval objects to be empty. Line 03 returns a list of ordered times when a line through  $Q_1$  or  $Q_2$  crosses a bucket corner vertex. Line 05 turns this list into a set of TimeInterval objects and adds them to the set of TimeIntervals. We list this "for each" loop as  $O(1)$  because it consists of a constant number of calculations bounded by the number of vertices in the bucket. Line 08 uses the linear time sorting algorithm BucketSort to sort the bucket time intervals. Line 09 creates the time partition order and index bucket time intervals from the bucket time intervals in  $O(B)$ . An additional pass adds the bucket time intervals to the appropriate index time intervals in  $O(B)$ . Lines 10-12 perform the Max-Count calculation discussed above.

In order to use the linear time BucketSort algorithm we need the following definition and lemmas.

Definition 3.10. We define the lexicographical ordering of two time intervals  $A$  and  $B$  as follows:

$$\begin{aligned}
 & A \prec B \text{ if } A \cdot l < B \cdot l \text{ or } (A \cdot l = B \cdot l \text{ and } A \cdot u < B \cdot u) \\
 & A \cdot l = B \cdot l \text{ and } A \cdot u = B \cdot u \text{ if } A = B
 \end{aligned}$$

The distribution of time interval objects created in Line 08 of the Max-Count algorithm may not be uniform across the query time interval  $T = [t^l; t^h]$ . However, we can still prove the following.



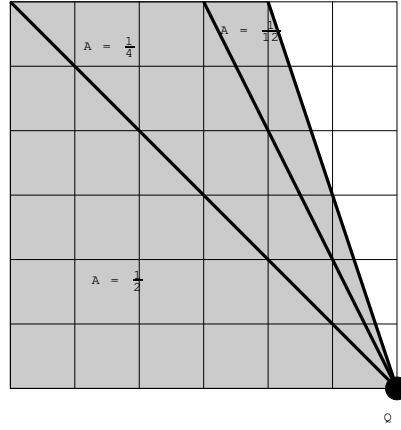


Fig. 16. Areas of Successive Slopes

Lemma 3.11. If the distribution of buckets is uniform, then the distribution of bucket time interval objects can be uniformly distributed within the sorting buckets of the bucket sort.

Proof. Consider the relationship between successive slopes measured as the angles between lines through a query point  $Q$  with slopes  $s_i = t_i$  and  $s_{i+1} = t_{i+1}$ . Suppose  $4t = 1$  with  $t_0 = 0$  and  $t_1 = 1$ , then the angle between the two lines is  $4s = \frac{\pi}{4}$ . The solid lines in Figure 16 show that half of the bucket corner vertices are swept by the line sweeping through  $Q$  between  $s_0 = 0$  and  $s_1 = 1$ . Consider a query time interval  $[0; 10]$ . Half of the corner vertices and thus half of the time intervals are between time  $t = 0$  and  $t = 1$ . Thus we conclude that the time interval objects created by sweeping will not be uniformly distributed throughout the query time interval.

Let  $Q^0$  be the midpoint between  $Q_1$  and  $Q_2$ , and  $S = [t_1; \dots; t_k]$  where  $t_1 = t^l$ ,  $t_k = t^r$  and each  $t_{i+1} - t_i = L$  for  $1 \leq i < k$ . Let  $D_B$  be a bucket that contains the space in the 6-dimensional index. Model the normalized bucket function for  $D_B$  as a constant  $F = 1$ . Thus  $p$ , the bucket probability, from (26) becomes the hyper-volume of the space swept by the line through  $Q^0$ . By Lemma 3.9 we can find the area for a specific time interval in  $S$  in constant time. The percentage of sorting buckets needed in any time interval  $T_i = [t_i; t_{i+1}] \subseteq S$  within the query time interval is given by:

$$\text{posb}_i = \frac{p(t_{i+1}) - p(t_i)}{p(t^r) - p(t^l)}$$

Let  $N$  be the number of sorting buckets. Then the number of sorting buckets assigned to interval  $i$  is given by:

$$\text{nosb}_i = N \cdot \text{posb}_i$$

If  $\text{nosb}_i < 1$  we can combine it with  $\text{nosb}_{i+1}$ . If the query time interval is very large, then we may need to include multiple time intervals from  $S$  to get one sorting bucket. Thus we create more sorting buckets (with smaller time intervals) in

areas where the expected number of bucket time intervals is large. Conversely, we create fewer sorting buckets (with larger time intervals) in areas where the expected number of bucket time intervals is small. Hence we model each sorting bucket so that its time interval length directly relates to the percentage of bucket time intervals that are assigned to it. Thus we conclude that we will uniformly distribute the time interval objects across all sorting buckets.  $\square$

**Lemma 3.12.** Insertion of any bucket time interval object  $T_0$  into the proper sorting bucket can be done in  $O(1)$  time.

**Proof.** The distribution of sorting buckets is determined by  $k$  time intervals in Lemma 3.11. Call these sorting time interval objects where each object contains: the lower bound  $l$ , the upper bound  $u$ , the number of sorting buckets assigned to this interval  $b_s$ , the length of the time interval for the sorting bucket  $w$  and an array  $B_p$  containing pointers to these sorting buckets. Let  $A$  be the array of sorting time interval objects, and  $L$  be the length of each time interval where the time intervals are as in Lemma 3.11. Then finding the correct sorting bucket for  $T_0$  requires two calculations:

$$\begin{aligned} \text{SortingTimeInterval} &= A \left\lfloor \frac{T_0.l}{L} \right\rfloor \\ \text{SortingBucket} &= B_p \left\lfloor \frac{T_0.l - \text{SortingTimeInterval}.l}{w} \right\rfloor \end{aligned}$$

Each of these requires constant time, hence  $T_0$  can be inserted into the proper sorting bucket in  $O(1)$  time.  $\square$

Using the above two lemmas, we can prove the following.

**Theorem 3.13.** The running time of the Max-Count algorithm is  $O(B)$  where  $B$  is the number of buckets.

**Proof.** Let  $H$  be the set of buckets where each bucket  $B_i$  contains the normalized trend function  $F_i$ . Let  $Q_1$  and  $Q_2$  be the query points and  $[t^l; t^u]$  be the query time interval. (Lines 01-07): Calculating the time intervals takes  $O(B)$  time because the cross times for each bucket can be calculated in constant time. (Line 08): By Lemma 3.11 and 3.12 we have an approximately even distribution of time interval objects within the sorting buckets where we can insert an object in constant time. This fulfills the requirements of the BucketSort [Cormen et al. 2001] which allows the intervals to be sorted in  $O(B)$  time. (Lines 09-12): Calculate the Max-Count and time for each time interval in constant time using Lemma 3.9. This takes  $O(B)$  time because there are  $O(B)$  time intervals. Finding the global Max-Count and time requires retaining the maximum time and count at line (11). Returning the Max-Count and time takes  $O(1)$  time. Thus the running time is given by  $O(B) + O(B) + O(B) + O(1) = O(B)$ .  $\square$

#### 4. AN EXACT MAX-COUNT ALGORITHM

Next we give a new algorithm which finds the exact Max-Count values.

---

Exact-Max-Count( $D; Q_1; Q_2; t^l; t^h$ )

input:  $D$  is the database of points. The query is made up of a hyper-rectangle  $Q$  defined by points  $Q_1$  and  $Q_2$  and the time interval  $T = [t^l; t^h]$

output: The exact Max-Count and time at which it occurs.

---

```

01. Times = ; of CrossTime objects                                O (1)
02. for each point  $p_i \in D$                                        O (N)
03.   if  $p_i \in Q$  during  $T$                                        O (1)
04.     EntryTime = CalculateEntryTime( $p_i; Q; T$ )                O (1)
05.     ExitTime = CalculateExitTime( $p_i; Q; T$ )                   O (1)
06.     if EntryTime  $\in$  Times                                       O (1)
07.       Times.get(EntryTime).Count++                             O (1)
08.     else
09.       Times.add(new CrossTime(EntryTime))                      O (1)
10.     end if
11.   if Times contains an object for ExitTime                     O (1)
12.     Times.get(ExitTime).Count--                                O (1)
13.   else
14.     Times.add(new CrossTime(ExitTime))                          O (1)
15.   end if
16. Sort(Times)                                                    O (N log N)
17. traverse Times while tracking time and Max-Count.              O (N)
18. return the time and Max-Count                                  O (1)

```

---

It is easy to see that the running time of the above algorithm is given by:

$$O(N) + O(n \log n) \quad (32)$$

where  $N$  is the number of points in the database and  $n$  represents the result size of the query.

It is possible to slightly improve the above algorithm. First, divide the index space into  $k$  subspaces and maintain separate partial databases for each. Assign processes on individual systems to each database to calculate the Max-Count query and return the time intervals to a central process. Merging the time interval lists into a global time interval list saves time on the sorting part of the algorithm. The running time for each of  $k$  partial databases would be close to  $O(\frac{n}{k} \log \frac{n}{k})$ . This is an approximate value because we do not guarantee an even split between databases. Placing buckets for each partial database in a tree structure may be reasonable and could cut down the average running time to  $O(\log N + n \log n/k)$ . Implementation and analysis for this particular approach is left as future work.

## 5. COUNT-RANGE ESTIMATION

**Definition 5.1.** Given a query rectangle  $R$  and a time interval  $t_{\text{interval}} = [t^l; t^h]$ , the Count-Range query returns the total number of points that intersect  $R$  in  $t_{\text{interval}}$ .

The Count-Range algorithm shown below is a simplification of Max-Count in that it is the Count portion of the Max-Count query.

---

Count-Range( $H; Q_1; Q_2; t^l; t^h$ )

input: A set of buckets  $H$  built by the index structure presented,  
query points  $Q_1(t)$  and  $Q_2(t)$  and a query time interval  $(t^l; t^h)$ .

output: the estimated Count-Range.

---

1.	For each bucket $B_i \in D$	$O(B)$
2.	Count = 0	$O(1)$
3.	If $B_i$ is completely contained in $Q$ during $T$	$O(1)$
4.	Count + $b_i$	$O(1)$
5.	If $B_i$ is partially contained in $Q$ during $T$	$O(1)$
6.	Calculate $p_i$ using (27)	$O(1)$
7.	Count + $\max(p_i(t^l; t^h))$	$O(1)$
8.	Return Count	$O(1)$

---

Theorem 5.2. The Count-Range query runs in  $O(B)$  time.

Proof. Consider two different data structures for our buckets: hash tables and R-trees. In the case of indexing using an R-tree, the worst case requires that we examine all buckets used in generating the Count-Range. It is possible that this could be all  $B$  buckets giving a worst case of  $O(B)$ . In the case of using a hash table, we must examine all  $B$  buckets. By Lemma 2.7 and the fact that (27) is calculated in constant time, each bucket can be examined to determine the count that contributes to the Count-Range query in constant time. Therefore the algorithm runs in  $O(B)$  time.  $\square$

## 6. THRESHOLD-RANGE ESTIMATION

Definition 6.1. Given a database of moving points  $D$ , a dynamic rectangle  $R$ , a threshold value  $M$  and a time interval  $[t_a; t_b]$ , the Threshold-Range returns a set of time intervals during which  $R$  contains  $M$  or more points.

The Threshold-Range algorithm shown below is related to Max-Count in the way we calculate the aggregation, and that it is a multi-level aggregation where a threshold is applied to a running count.

---

Threshold-Range( $H; Q_1; Q_2; t^l; t^h; M$ )

input: A set of buckets  $H$  build by the index structure presented,  
 query points  $Q_1(t)$  and  $Q_2(t)$ , a query time interval  $[t^l; t^h]$ ,  
 and  $M$  is the threshold value

output: The estimated set of time intervals where  $R$  contains more  
 than  $M$  points.

01 – 08 are the same as the Max-Count algorithm.

```

09.  TimeIntervals = ;                                O(1)
10.  For each TimeInterval2 TimePartitionOrder      O(B)
11.      CM axCount = calculate(M axCount; M axTime; TimeInterval) O(1)
12.      if CM axCount > M                            O(1)
13.          TimeIntervals = TimeIntervals  $\cup$  TimeInterval O(1)
14.  Merge(TimeIntervals)                             O(B)
15.  return TimeIntervals

```

---

Theorem 6.2. The estimated Threshold-Range query runs in  $O(B)$  time.

Proof. The Threshold-Range algorithm differs from the Max-Count algorithm only in lines 09-15. Lines 11-13 run in  $O(1)$  time. Line 10 executes lines 11-13  $O(B)$  times. In line 14, Merge(TimeIntervals) is a linear walk of the time intervals which joins adjacent time intervals  $T_a$  and  $T_b$  when  $T_a \cup T_b$  would form a continuous time interval. The calculation is trivially  $O(1)$  time for joining the adjacent intervals. Hence we conclude by Theorem 3.13 that the Threshold-Range runs in  $O(B)$  time.  $\square$

We suggest the following three variations of Threshold-Range and note that neither variation changes the running time from the Threshold-Range algorithm.

**Threshold-Count:** By adding a line between 14 and 15 in the Threshold-Range algorithm that counts the merged time intervals, we can return the count of time intervals during the query time interval where congestion occurs. This gives a measure of variation in congestion.

**Threshold-Average:** By adding a line between 14 and 15 in the Threshold-Range algorithm that finds average length of the merged time intervals, we can return the average length of time each congestion will last. This gives a measure of the severity of each congestion.

**Threshold-Sum:** By summing the times instead of using the  $\cup$  operator in line 13 of the Threshold-Range algorithm, we can return the total congestion time during the query time interval. This gives a measure of the severity of congestion that may be compared to the length of query time.

## 7. EXPERIMENTAL RESULTS

In the following experimental analysis, we measure the accuracy of the estimation algorithm relative to the exact-count algorithm as follows:

$$\text{Accuracy}_{\text{relative}} = \frac{|\text{Exact Max Count} - \text{Estimated Max Count}|}{\text{Exact Max Count}} \quad (33)$$

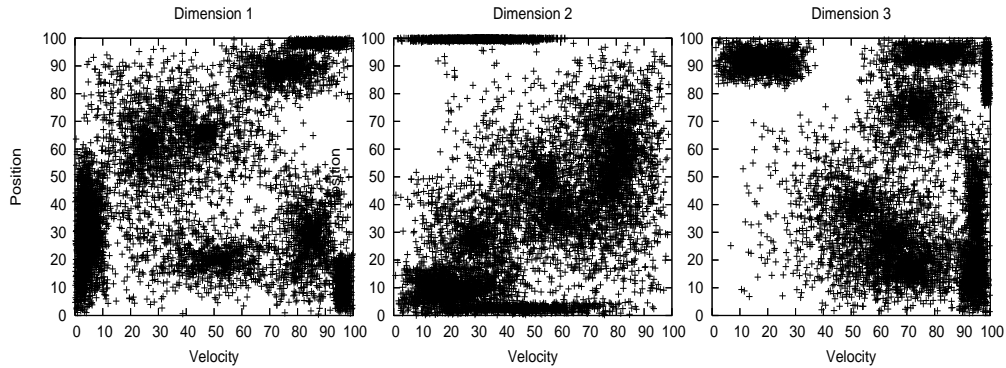


Fig. 17. Sample Data View

This is a useful measure if the query returns a reasonable number of points. Queries that return a very small number of points would skew the results and are not included.

Data for the experiments was randomly generated around several cluster centers. The  $i^{\text{th}}$  point generated for the database is located near a randomly selected cluster at a distance between 0 and  $d$ , where  $d$  is proportional to  $i$ . A single cluster near a corner would approximate the Zipf distribution used in [Choi and Chung 2002; Revesz and Chen 2003; Tao et al. 2003b]. Figure 17 shows a sample of a database with points projected onto the three views.

### 7.1 Parameters Effects

The index space went from 0 to 100 in each dimension. The number of points in the different data sets ranged from 500,000 to 1,500,000. The following parameters were used in creating the index and finding the Max-Count.

**Size of Buckets:** The size of the buckets determines the number of possible buckets in the index. In the experiments, buckets divide the space up such that there are 10 to 40 divisions in each dimension. This equates to bucket sizes ranging from 2.5 to 10 units wide in each dimension. Relative to our previous work [Anderson 2006] this puts much more space into each bucket creating bigger buckets.

**Cluster Points:** Index space saturation determines the number of buckets necessary for the index. The number of cluster points does not appear to affect point saturation or error as much as the space saturation.

**Histogram Divisions:** Increasing histogram divisions to  $s > 5$  had no effect on the accuracy. This is not unexpected because histograms are used to define a trend function relative to one another. Increasing the histogram divisions has a tendency to flatten the lines. However, normalization flattens the trend function while maintaining the trends so this behavior is easily explained. Hence increasing histogram divisions only increases the running time without increasing accuracy.

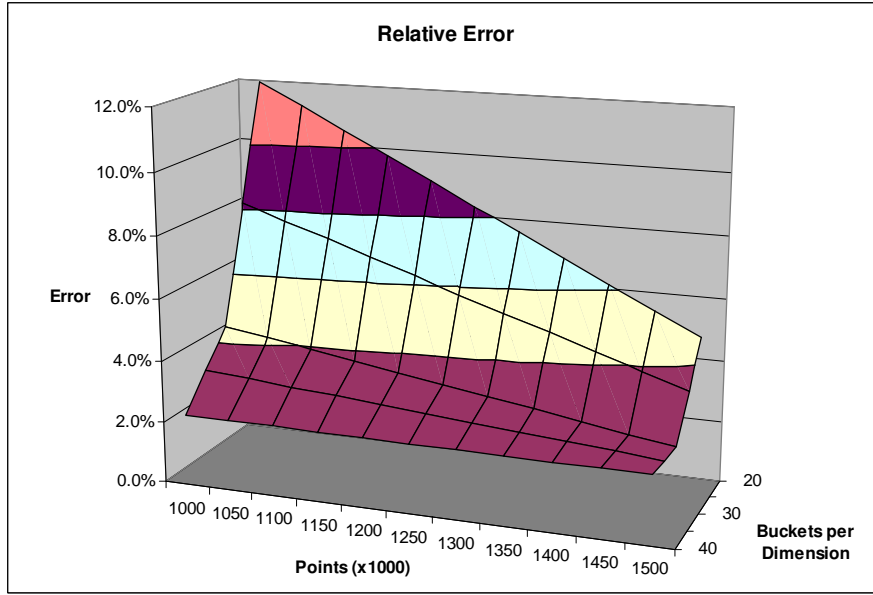


Fig. 18. Relative Error

## 7.2 Observations: Estimated Max-Count

When dealing with either very small or very large time end points the method is susceptible to rounding error. In particular, the volume function contains both  $t^6$  and  $\frac{1}{t^6}$  terms. For very small time values these calculations are extremely sensitive and care must be given to guard against rounding error. These errors showed in two ways. First by a direct warning programmed into the solution and second by a series of fairly stable time values for the Max-Count followed by unstable variations when increasing the number of buckets. At some point smaller bucket sizes increases the likelihood of errors in both time and count values. As the bucket size becomes smaller in successive runs, the existence of instability in the time values after a series of stable values predicts that an extremely accurate Max-Count may be found in the previous larger bucket size. Throughout our experiments, this was an excellent predictor of an accurate Max-Count.

The experiments demonstrated that 6-dimensional space compounds the problem of creating sufficiently small buckets. Creating an index with unit buckets would result in the possibility of having  $1 \cdot 10^{12}$  buckets. Clearly this is unrealistic for common moving object applications where we may be dealing with 1 to 10 million objects of interest. In practice the number of buckets needed to reach acceptable error levels was between 78,000 and 227,000 buckets. These numbers reflect the ability to reach error levels under 5% and were roughly related to the saturation of the space by the points.

Figure 18 shows that increasing the number of buckets to the indicated values dramatically decreases the error. As the number of points increases we also see a near linear decrease in the error. Note that for larger buckets (e.g. smaller values

on the "Buckets per Dimension axis"), the decrease in error is more dramatic.

### 7.3 Exact vs. Estimated Max-Count

The exact Max-Count provided the values against which our estimation algorithm was tested for accuracy. Since the method does not rely on buckets, and has zero error we note only that on queries with very small query result sizes, this method performs well.

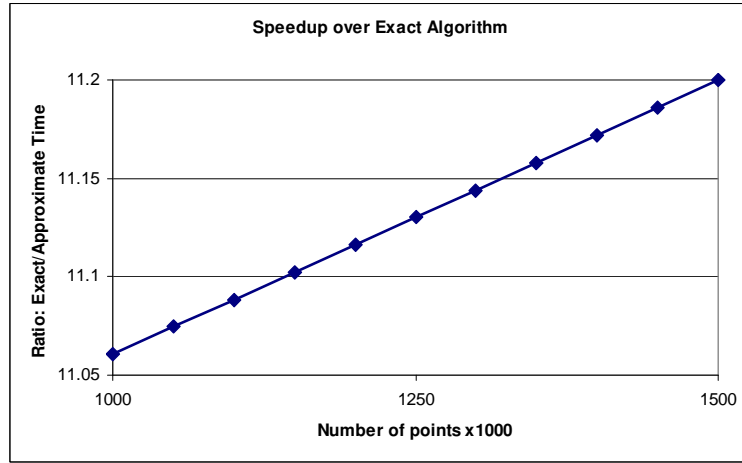


Fig. 19. Ratio of Exact Running Time to Estimated Running Time

Figure 19 shows the average ratio of the exact Max-Count running time to the estimated Max-Count running time as a function of the number of points in the database. This shows a very stable, but small linear growth in speedup with databases of sizes between 1 to 1.5 million points.

A natural question is when to use the exact versus the estimated method for Max-Count. In runs with a small number of points returned by a Max-Count query, the two methods run about equally fast. However when the result size reaches values greater than 20,000 the estimated Max-Count runs up to 35 times faster than the exact Max-Count algorithm.

## 8. CONCLUSIONS

We implemented and compared two new Max-Count algorithms. The estimated Max-Count was shown to be fast and accurate while still allowing fast constant time updates. No other algorithm has these features to date. We showed that Threshold-Range with its variations and Count-Range are related to Max-Count and can be evaluated using the same techniques and that we expect similar or better accuracy in these operations. We gave an empirical threshold for choosing between the exact and estimated Max-Count algorithms. We discussed the issues related to higher dimensions and showed that all sweeping algorithms have this problem. We also note that using our technique it is possible to decompose the



problem and run it in a multiprocessor or grid environment where the database is divided into smaller databases.

Future work may include decreasing the running time by finding other techniques because there does not appear to be a clear method for decreasing the running time of sweeping methods. One could also consider implementing and comparing these techniques in a grid environment.

#### REFERENCES

- Acharya, S., Poosala, V., and Ramaswamy, S. 1999. Selectivity estimation in spatial databases. In *Proceedings of the ACM SIGMOD International Conference on Management of Data*. ACM Press, New York, NY, USA, 13{24.
- Agarwal, P. K., Arge, L., and Erickson, J. 2003. Indexing moving points. *Journal of Computer and System Sciences* 66, 1, 207{243.
- Anderson, S. 2006. Aggregation estimation for 2d moving points. In *Thirteenth International Symposium on Temporal Representation and Reasoning*. IEEE Computer Society Press, Piscataway, NJ, USA, 137{144.
- Beckmann, N., Kriegel, H. P., Schneider, R., and Seeger, B. 1990. The R-tree: An efficient and robust Access Method for Points and Rectangles. In *Proceedings of ACM /SIGMOD Annual Conference on Management of Data (SIGMOD)*. 322{331.
- Bohlen, M. H., Gamber, J., and Jensen, C. S. 2006. How would you like to aggregate your temporal data? In *Thirteenth International Symposium on Temporal Representation and Reasoning*. 121{136.
- Cai, M. and Revesz, P. 2000. Parametric R-tree: An index structure for moving objects. In *Proceedings of the 10th COMAD International Conference on Management of Data*. Tata McGraw-Hill, 57{64.
- Chen, Y. and Revesz, P. 2004. Max-count aggregation estimation for moving points. In *Proceedings of the 11th International Symposium on Temporal Representation and Reasoning*. 103{108.
- Choi, Y.-J. and Chung, C.-W. 2002. Selectivity estimation for spatio-temporal queries to moving objects. In *Proceedings of the ACM SIGMOD International Conference on Management of Data*. 440{451.
- Civilis, A., Jensen, C. S., Nenortaitė, J., and Pakalnis, S. 2004. Efficient tracking of moving objects with precision guarantees.  *ubiquitous* 00, 164{173.
- Civilis, A., Jensen, C. S., and Pakalnis, S. 2005. Techniques for efficient road-network-based tracking of moving objects. *IEEE Transactions on Knowledge and Data Engineering* 17, 5, 698{712.
- Cormen, T. H., Leiserson, C. E., Rivest, R. L., and Stein, C. 2001. *Introduction to Algorithms*, 2nd ed. MIT Press, Massachusetts.
- Gunopulos, D., Kollios, G., Tsotras, J., and Domeniconi, C. 2005. Selectivity estimators for multidimensional range queries over real attributes. *The VLDB Journal* 14, 2, 137{154.
- Gupta, S., Kopparty, S., and Ravishankar, C. V. 2004. Roads, codes and spatiotemporal queries. In *Proceedings of the ACM SIGMOD-SIGACT-SIGART Symposium on Principles of Database Systems*. 115{124. gave a technique for answering spatiotemporal range, intercept, incidence and shortest path queries on objects that move along curves in a planar graph.
- Guting, R. H. and Schneider, M. 2005. *Moving Objects Databases*. Morgan Kaufmann.
- Guttman, A. 1984. R-trees: A dynamic index structure for spatial searching. In *Proceedings of the ACM SIGMOD International Conference on Management of Data*, B. York, Ed. ACM Press, 47{57.
- Kollios, G., Gunopulos, D., and Tsotras, V. J. 1999. On indexing mobile objects. In *Proceedings of the eighteenth ACM SIGMOD-SIGACT-SIGART Symposium on Principles of Database Systems*. 261{272.
- Kollios, G., Papadopoulos, D., Gunopulos, D., and Tsotras, J. 2005. Indexing mobile objects using dual transformations. *The VLDB Journal* 14, 2, 238{256.

- Mokhtar, H., Su, J., and Ibarra, O. 2002. On moving object queries: (extended abstract). In *Proceedings of the 21st ACM SIGMOD-SIGACT-SIGART Symposium on Principles of Database Systems*. 188{198.
- Papadopoulos, D., Kollios, G., Gunopulos, D., and Tsotras, V. J. 2002. Indexing mobile objects on the plane. In *Proceedings of the International Conference on Database and Expert Systems Applications*. Aix en Provence, France.
- Pelania, M., Saltenis, S., and Jensen, C. S. 2006. Indexing the past, present, and anticipated future positions of moving objects. *ACM Trans. Database Syst.* 31, 1, 255{298.
- Porkaew, K., Lazaridis, I., and Mehrotra, S. 2001. Querying Mobile Objects in Spatio-Temporal Databases. In *Proceedings of Symposium on Spatial and Temporal Databases (SSTD)*. 59{78.
- Revesz, P. 2005. Efficient rectangle indexing algorithms based on point dominance. In *Proceedings of the 12th International Symposium on Temporal Representation and Reasoning*. IEEE Computer Society Press.
- Revesz, P. and Chen, Y. 2003. Efficient aggregation over moving objects. In *Proceedings of the 10th International Symposium on Temporal Representation and Reasoning, Fourth International Conference on Temporal Logic*. 118{127.
- Rigaux, P., Scholl, M., and Voisard, A. 2001. *Spatial Databases: With Applications to GIS*. Morgan Kaufmann Publishers, San Francisco, CA, USA.
- Saltenis, S., Jensen, C. S., Leutenegger, S. T., and Lopez, M. A. 2000. Indexing the positions of continuously moving objects. In *Proceedings of the ACM SIGMOD International Conference on Management of Data*. 331{342.
- Samet, H. 1990. *The design and analysis of spatial data structures*. Addison-Wesley Longman Publishing Co., Inc., Boston, MA, USA.
- Samet, H. 2005. *Foundations of Multidimensional and Metric Data Structures*. Morgan Kaufmann Publishers, San Francisco, CA.
- Tao, Y. and Papadias, D. 2005. Historical spatio-temporal aggregation. *ACM Trans. Inf. Syst.* 23, 1, 61{102.
- Tao, Y., Sun, J., and Papadias, D. 2003a. Selectivity estimation for predictive spatio-temporal queries. In *Data Engineering, 2003. Proceedings. 19th International Conference on*. 417{428. Nothing new over previous selectivity estimation paper. Still dealing with query optimization.
- Tao, Y., Sun, J., and Papadias, D. 2003b. Selectivity estimation for predictive spatio-temporal queries. In *Proceedings of the 19th International Conference on Data Engineering*.
- Tayeb, J., Ulusoy, O., and Wolfson, O. 1998. A quadtree-based dynamic attribute indexing method. *Comput. J.* 41, 3, 185{200. This is a very preliminary work, probably the first of its kind and talks about two types of queries: instantaneous and continuous(ly repeated) types. This is a horizon paper...
- Trajcevski, G., Wolfson, O., Hinrichs, K., and Chamberlain, S. 2004. Managing uncertainty in moving objects databases. *ACM Trans. Database Syst.* 29, 3, 463{507.
- Wolfson, O. and Yin, H. 2003. Accuracy and resource consumption in tracking and location prediction. In *Proceedings of the Symposium on Spatial and Temporal Databases (SSTD)*. 325{343.
- Zhang, D., Gunopulos, D., Tsotras, V. J., and Seeger, B. 2003. Temporal and spatio-temporal aggregations over data streams using multiple time granularities. *Inf. Syst.* 28, 1-2, 61{84.
- Zhang, D., Markowetz, A., Tsotras, V., Gunopulos, D., and Seeger, B. 2001. Efficient computation of temporal aggregates with range predicates. In *Proceedings of the twentieth ACM SIGMOD-SIGACT-SIGART Symposium on Principles of Database Systems*. 237{245.

...